Applied Catalysis B: Environmental 88 (2009) 83–97

Contents lists available at ScienceDirect

Applied Catalysis B: Environmental

journal homepage: www.elsevier.com/locate/apcatb

Factors influencing structure and catalytic activity of $Au/Ce_{1-x}Zr_xO_2$ catalysts in CO oxidation

Izabela Dobrosz-Gómez [1], Ireneusz Kocemba, Jacek M. Rynkowski *

Institute of General and Ecological Chemistry, Technical University of Łódź, Żeromskiego 116, 90-924 Łódź, Poland

ARTICLE INFO

Article history:
Received 17 June 2008
Received in revised form 14 September 2008
Accepted 19 September 2008
Available online 9 October 2008

Keywords:
$Au/Ce_{1-x}Zr_xO_2$ catalyst
Preparation procedure
Residual chlorine
Au dispersion
CO oxidation

ABSTRACT

The $Au/Ce_{1-x}Zr_xO_2$ ($x = 0, 0.25, 0.5, 0.75, 1$) catalysts were synthesized by the direct anionic exchange (DAE) method, characterized by BET, SEM–EDS, XRD, TPR-CO, HRTEM, AAS, ToF-SIMS and tested in CO oxidation. The correlations between structural, redox and catalytic properties of $Au/Ce_{1-x}Zr_xO_2$ catalysts prepared using different synthesis procedures have been studied. The poisoning effect of residual chlorine on their catalytic performance was found. The agglomeration of Au particles during the calcination step in the presence of residual chlorine was observed. Its removal through the washing treatment both inhibited the sintering process and led to the increase in activity of the studied systems. The sequence of increasing activity was followed by the sequence of increasing reducibility of the catalysts. This shows the role of the support redox properties in the creation of the catalytic performance of supported Au nanoparticles in CO oxidation.

1. Introduction

Gold catalysts have recently been attracting a rapidly growing interest due to their potential applications in many reactions, of both industrial and environmental importance [1,2]. Among these reactions, oxidation of carbon monoxide is an important one.

Various parameters, including the Au precursor, the nature of the support, the temperature and atmosphere of catalysts activation, the reaction conditions, and particularly the size of gold clusters, have already been considered as crucial factors influencing the chemistry, structure, and catalytic activity of gold-containing systems [1–5]. Beside these factors, the importance of the support in the creation of their catalytic performance must be emphasized. According to the literature [1,6], the role of the support in the stabilization of the active phase dispersion and modification of its electronic state is significant. Furthermore, its participation in the activation of reactants, especially oxygen has been suggested [7–10]. Despite of the extensive research work on Au catalysts design and characterization, the CO oxidation mechanism and the role of the oxide support in the reaction are still under debate. At present, the exact effect of the residual chlorine on the catalytic performance of Au catalysts in CO oxidation is not completely understood. Its poisonous effect e.g., in Au/TiO_2 [11] and Au/Al_2O_3 [12] is well established. The residual chlorine was found to facilitate the agglomeration of Au particles during the heat treatment through the formation of Au–Cl–Au bridges and to inhibit the catalytic activity by poisoning the catalysts active sites [13]. According to Kung et al. [14], in the case of Au/Al_2O_3 catalyst, chloride in the amount of Cl/Au atom ratio of 0.1 would decrease the activity approximately by a half. We also demonstrated the poisonous effect of the residual chlorine on the catalytic activity of Au/Mg_4Al_2 in CO oxidation [3]. Recently, Qiao and Deng [15] showed that the presence of Cl^- in $Au–Au^+–Cl_x/Fe(OH)_y$ catalyst slightly affects the activity in selective CO oxidation over the unwashed and uncalcined catalysts. They indicated that the presence of hydroxyl species in the uncalcined, chloride-containing catalysts can be responsible for the weakened interactions between Au species and Cl^-, resulting in quite high activity towards CO oxidation. However, after calcination at 400 °C, the activity of $Au–Au^+–Cl_x/Fe(OH)_y$ system in CO oxidation was significantly reduced. On the other hand, in the case of Au/MCM-41 catalyst [16], chloride ions were found to serve as a catalytically active basic species in the acetonylacetone transformation. Such activity was possible due to the weak Au–Cl interactions. As it could be seen, the different effects of residual chlorine on the activity of Au catalysts strongly depend on the oxide support, the

* Corresponding author. Tel.: +48 42 6313117; fax: +48 42 6313128.
E-mail address: jacryn@p.lodz.pl (J.M. Rynkowski).
[1] Present address: Facultad de Ciencias Exactas y Naturales, Universidad Nacional de Colombia, Sede Manizales, Colombia.

0926-3373/$ – see front matter © 2008 Elsevier B.V. All rights reserved.
doi:10.1016/j.apcatb.2008.09.028

catalyst temperature treatment, etc. It confirms that better understanding of the role of Cl^- can improve a control of variables important in Au catalysts preparation.

In our previous paper [17] the usefulness of CeO_2–ZrO_2 mixed oxides, CeO_2 and ZrO_2 as supports for Au nanoparticles has been studied, mainly from the point of view their contribution to the reaction. As ceria–zirconia supported Au catalysts appeared to be very promising, we believe that a more detailed insight into the different factors controlling their structure and activity is worth of efforts and publication. Thus, the effects of the preparation procedure and the physico-chemical properties of the oxide supports on the catalytic activity of $Au/Ce_{1-x}Zr_xO_2$ catalysts in CO oxidation are presented in details. A special attention is paid to the influence of residual chlorine in the catalysts on their properties and catalytic performance. The $Au/Ce_{1-x}Zr_xO_2$ catalysts were synthesized, characterized by BET, SEM–EDS, XRD, TPR-CO, HRTEM, AAS, ToF-SIMS and tested in CO oxidation. The correlations between structural, redox and catalytic properties of $Au/Ce_{1-x}Zr_xO_2$ systems are discussed.

2. Experimental

2.1. Synthesis

A series of $Ce_{1-x}Zr_xO_2$ (x = 0.25, 0.5, 0.75) solid solutions, CeO_2 and ZrO_2 used as a support for Au was prepared by the sol–gel like method using as the starting materials, zirconium(IV) acetylacetonate [$Zr(CH_3COCH_2COCH_3)_4$, Avocado, purity 99.9%] and/or cerium(III) acetyloacetonatehydrate [$Ce(CH_3COCH_2COCH_3)_3{\cdot}H_2O$, Sigma–Aldrich, purity 99.9%] and calcined at 550 °C, in details described previously [17].

Hydrogen tetrachloroaureate(III) trihydrate [$HAuCl_4{\cdot}3H_2O$, Sigma–Aldrich, purity 99.9%] was used as a gold precursor. The catalysts were prepared by the direct anionic exchange (DAE) method of gold species with hydroxyl groups of the support [3,18]. The optimisation of catalyst synthesis conditions was presented previously [19]. Aqueous solution of $HAuCl_4$ at the concentration 2.25×10^{-4} M was prepared using 900 cm^3 of distilled water. The solution was heated up to 70 °C and the support was introduced. After 1 h of thermostating and vigorous stirring, the suspension was centrifuged. In order to remove the residual chlorine from the catalysts, two washing procedures prior to the drying process were applied. Depending on the washing procedure, the solids were suspended in either 4 M ammonia solution at 25 °C or deionised water at 50 °C and stirred for 1 h and next centrifuged again. After drying in an oven at 120 °C overnight, the catalysts were calcined in air at 300 °C for 4 h.

2.2. Characterization methods

Nitrogen adsorption/desorption isotherms at −196 °C were measured using Sorptomatic 1900 apparatus (Carlo-Erba). Prior to the measurement, all samples were degassed for 4 h at 250 °C. The specific surface area, S_{BET} was calculated using BET equation.

Atomic absorption spectroscopy (AAS) analyses were performed with a Solaar M6 Unicam spectrophotometer in order to estimate the amount of Au deposited on supports, in details described previously [17].

X-ray diffraction (XRD) patterns were obtained at room temperature using a PANalytical X'Pert Pro MPD diffractometer, operating at 40 kV and 30 mA (Cu K_α radiation). Data were collected in the range 20–70° 2θ with a step size of 0.0167° and step time of 10 s. JCPDS files were used for the identification of the diffraction peaks. The particle size ($D_{h\,k\,l}$) was estimated using the Scherer equation, as described previously [17].

High-resolution transmission electron microscopy (HRTEM) measurements were carried out using high-resolution microscope EM-002B (TOPCON), at an acceleration voltage 200 kV, equipped with energy-dispersive spectrometer (EDS). To determine an average Au particle size and to define their distribution more accurate, at least 500 particles of each catalyst were chosen. Moreover, many different HRTEM images of each catalyst sample have been analysed, in details described previously [3,17].

Scanning electron microscopy (SEM) measurements were performed by S-4700 microscope (Hitachi, Japan), using an acceleration voltage 20 kV, equipped with energy-dispersive spectrometer (EDS) (Thermo Noran, USA). An attempt to estimate the dispersion of Au was undertaken using the images recorded with the back-scattered electron (BSE) YAG-type detector [17].

ToF-SIMS measurements [20] were performed using an ION-ToF (GmbH) instrument (ToF-SIMS IV) equipped with 25 kV pulsed $^{69}Ga^+$ primary ion gun in the static mode. To obtain the plain surface of catalysts, powder samples were tableted before the measurements. The analysed area corresponds to a square of 500 μm × 500 μm in the case of spectra collecting and surface imaging. For each sample three spectra were made from different surface areas.

Temperature-programmed reduction (TPR-CO) measurements were carried out by PEAK-4 apparatus, using CO as reducing agent. The apparatus was equipped with an infrared gas analyser (Fuji Electric Systems Co., type: ZRJ-4) to analyse CO_2 formation. TPR-CO experiments were performed using a CO/He (5 vol.% CO, 95 vol.% He) gas mixture, with a flow rate of 40 $cm^3\,min^{-1}$, in the temperature range 25–850 °C, with a ramp rate 15 °C min^{-1}. Powdered samples of 100 mg were exposed to dry Ar at 250 °C for 1 h before the reduction. Based on the CO_2 formation, reduction degrees of the investigated samples were calculated, in details described previously [17].

CO oxidation reaction was carried out at atmospheric pressure in a quartz flow microreactor containing 100 mg of sample in a fixed bed, using a series of mass flow controllers with diluted gases. Before the reaction, a pretreatment in air at 300 °C for 1 h with a ramp rate of 5 °C min^{-1} was carried out. The gas mixture containing 1.6 vol.% CO and 3.3 vol.% O_2 (He as an eluant gas) was used with a flow of 50 $cm^3\,min^{-1}$, in the temperature range 25–300 °C, with a ramp rate 5 °C min^{-1}. The catalytic experiments were repeated several times in order to verify their reproducibility. Gas chromatograph fitted with molecular sieves 5 Å, equipped with a thermal conductivity detector was used to perform the analysis of both CO and O_2 concentration [21]. The catalytic performance was assessed in terms of both T_{10} and T_{50} temperatures, defined as the temperature at which 10% and 50% CO conversion was obtained, respectively.

3. Results and discussion

3.1. Textural and morphological characterization

Table 1 presents the specific surface area, the real Au loading and the Au particle size of $2Au/Ce_{1-x}Zr_xO_2$ catalysts prepared using different synthesis procedures.

The catalysts as prepared (without washing) show the real Au content almost identical to the nominal one, except for the catalyst supported on zirconia, which presents the real Au loading ca. 20% lower than the expected one. As we discussed earlier [17], the lower amount of Au exchanged with ZrO_2 oxide can be ascribed to the much lower specific surface area of ZrO_2 comparing to the CeO_2 and Ce–Zr mixed oxides (Table 1). The chemical analysis shows that washing of the catalysts with either warm water or ammonia leads to a loss of Au (ca. 5–10% for the catalysts washed with warm

Table 1
Characterization of oxide supports and $2Au/Ce_{1-x}Zr_xO_2$ catalysts washed with different agents.

Oxide supports/catalyst denotation (the first number corresponds to the nominal wt.% content of Au)	Real gold loading[a] (wt.%)	Surface area[b] ($m^2\ g^{-1}$)	Au particle size[c] (nm)	$D_{oxide\ support}$[d] (nm)
CeO_2	–	58.1	–	14.2 Ce(1 1 1)
$Ce_{0.75}Zr_{0.25}O_2$	–	50.1	–	7.0 Ce(1 1 1)
$Ce_{0.5}Zr_{0.5}O_2$	–	46.5	–	6.4 Ce(1 0 1)
$Ce_{0.25}Zr_{0.75}O_2$	–	41.0	–	6.7 Ce(1 0 1)
ZrO_2	–	4.5	–	23.4 Zr(−1 1 1), 19.0 Zr(1 0 1)
Without washing				
$2Au/CeO_2$	1.99	50	15.9	12.3 Ce(1 1 1)
$2Au/Ce_{0.75}Zr_{0.25}O_2$	1.98	46.5	15.7	6.7 Ce(1 1 1)
$2Au/Ce_{0.5}Zr_{0.5}O_2$	1.98	42.5	–	6.2 Ce(1 0 1)
$2Au/Ce_{0.25}Zr_{0.75}O_2$	1.98	38.9	–	6.6 Ce(1 0 1)
$2Au/ZrO_2$	1.65	2.8	19.5	21.9 Zr(−1 1 1), 15.9 Zr(1 0 1)
Washed with warm water				
$2Au/CeO_2$	1.89	51	11.3	13.5 Ce(1 1 1)
$2Au/Ce_{0.75}Zr_{0.25}O_2$	1.84	47.9	11.1	6.9 Ce(1 1 1)
$2Au/Ce_{0.5}Zr_{0.5}O_2$	1.86	43.8	–	6.3 Ce(1 0 1)
$2Au/Ce_{0.25}Zr_{0.75}O_2$	1.83	39.9	–	6.8 Ce(1 0 1)
$2Au/ZrO_2$	1.52	3.1	14.2	22.2 Zr(−1 1 1), 18.0 Zr(1 0 1)
Washed with ammonia				
$2Au/CeO_2$	1.79	51.5	4.0	6.4 Ce(1 1 1)
$2Au/Ce_{0.75}Zr_{0.25}O_2$	1.68	49.5	3.9	7.2 Ce(1 1 1)
$2Au/Ce_{0.5}Zr_{0.5}O_2$	1.74	45	–	6.7 Ce(1 0 1)
$2Au/Ce_{0.25}Zr_{0.75}O_2$	1.71	40.7	–	7.0 Ce(1 0 1)
$2Au/ZrO_2$	1.45	3.8	5.6	27.8 Zr(−1 1 1), 18.8 Zr(1 0 1)

D_{Au}, average diameter of Au particles; $D_{oxide\ support}$, the crystallite size of the oxide support.
[a] Determined by AAS.
[b] Determined by N_2-BET.
[c] Determined by HRTEM.
[d] Determined by XRD.

water and ca. 10–15% with ammonia), comparing to those prepared without the washing stage. This loss of Au is attributed to the removal of non-attached gold complexes, simply adsorbed on the support surface due to the deficient quantity of hydroxyl groups which are available for anionic exchange. Moreover, during the washing of the catalysts with ammonia, this effect is strengthened by the replacement of Cl^- ligands by OH groups in the exchanged Au species [22]. It should be noted that the removal of residual chlorine with ammonia is highly efficient. Its amount in e.g., Au/Mg_4Al_2 [3] and Au/CeO_2 [23] was found to be lower than 200 ppm.

The specific surface area of $2Au/Ce_{1-x}Zr_xO_2$ ($x = 0$, 0.25, 0.5, 0.75) catalysts is in the range 39–52 m^2/g, except for the $2Au/ZrO_2$ one having the specific surface area significantly lower (Table 1). In general, washing of the catalyst with warm water or ammonia does not lead to considerable change in its BET surface area.

$Ce_{1-x}Zr_xO_2$ oxides prepared by the sol–gel method are highly uniform and the strong effect of the oxide composition on their morphology was confirmed by SEM–EDS technique [17]. The interaction of Au precursor ($HAuCl_4{\cdot}3H_2O$) with CeO_2 surface during the catalyst preparation does not lead to the aggregation of spherical grains of the oxide support. Neither agglomeration of regular and plated shaped particles of $Ce_{0.75}Zr_{0.25}O_2$ (Fig. 1a) nor angular particles of ZrO_2 are observed. The morphology of supported Au catalysts strongly depends on the composition of the oxide supports. The BSE photomicrographs and EDS maps confirm rather high Au dispersion on all oxides. However, the presence of some microareas corresponding to the higher Au concentration, with the size of around 1 μm is clearly visible. The Au clusters were found as well (Fig. 1a). The number of counts characteristic of chloride ions in the X-ray spectra is higher for $2Au/CeO_2$ and $2Au/Ce_{0.75}Zr_{0.25}O_2$ than for $2Au/ZrO_2$, probably as a result of higher affinity of ceria to chlorine. In fact, the existence of CeO_2–Cl species in Au/CeO_2 sample was reported previously [24].

In the case of the catalysts prepared without washing, the dispersion of Au depends on the pretreatment temperature. As we mentioned above, for the samples calcined at 300 °C the characteristic microareas with the higher Au concentration are observed (Fig. 1a). However, for the uncalcined catalysts a more homogenous distribution of Au particles on the surface is recorded (Fig. 1b). It confirms the possibility of Au particles agglomeration during the calcination step, probably due to the creation of Au–Cl–Au bridges, as suggested by Schulz and Hargittai [13].

Washing of the studied catalyst with warm water does not change the characteristic picture of the oxide supports particles. However, in contrast to the catalysts prepared without washing, a more homogenous distribution of Au on the support surface is observed (Fig. 2a). The microareas responding to the higher Au concentration become almost not visible, as confirmed by the BSE photomicrographs and EDS maps. No Au clusters were found. The application of warm water as a washing agent leads to the decrease in the residual chlorine content in the catalysts, as we reported previously [3]. However, the signal characteristic of Cl^- in the X-ray spectrum of $2Au/CeO_2$ (not presented here) was still visible, while it was not present in the X-ray spectra of both $2Au/Ce_{0.75}Zr_{0.25}O_2$ (Fig. 2a) and $2Au/ZrO_2$ (not presented here) catalysts. The higher quantity of residual chlorine after washing with warm water was also found for Au/CeO_2 catalyst, compared with Au/ZrO_2 one [23]. Washing of $2Au/CeO_2$ catalyst with ammonia leads to a decrease in the spherical grain size of the oxide (BSE photomicrograph not presented here) [17]. However, such effect is observed neither for regular and plated shaped particles of $Ce_{0.75}Zr_{0.25}O_2$ nor for angular particles of ZrO_2. In contrast to the catalysts prepared without washing, a homogenous distribution of Au on the supports surface is observed (Fig. 2b). Distribution of Au As confirmed by the BSE photomicrographs and EDS maps, neither the microareas corresponding to the higher Au concentration nor Au clusters

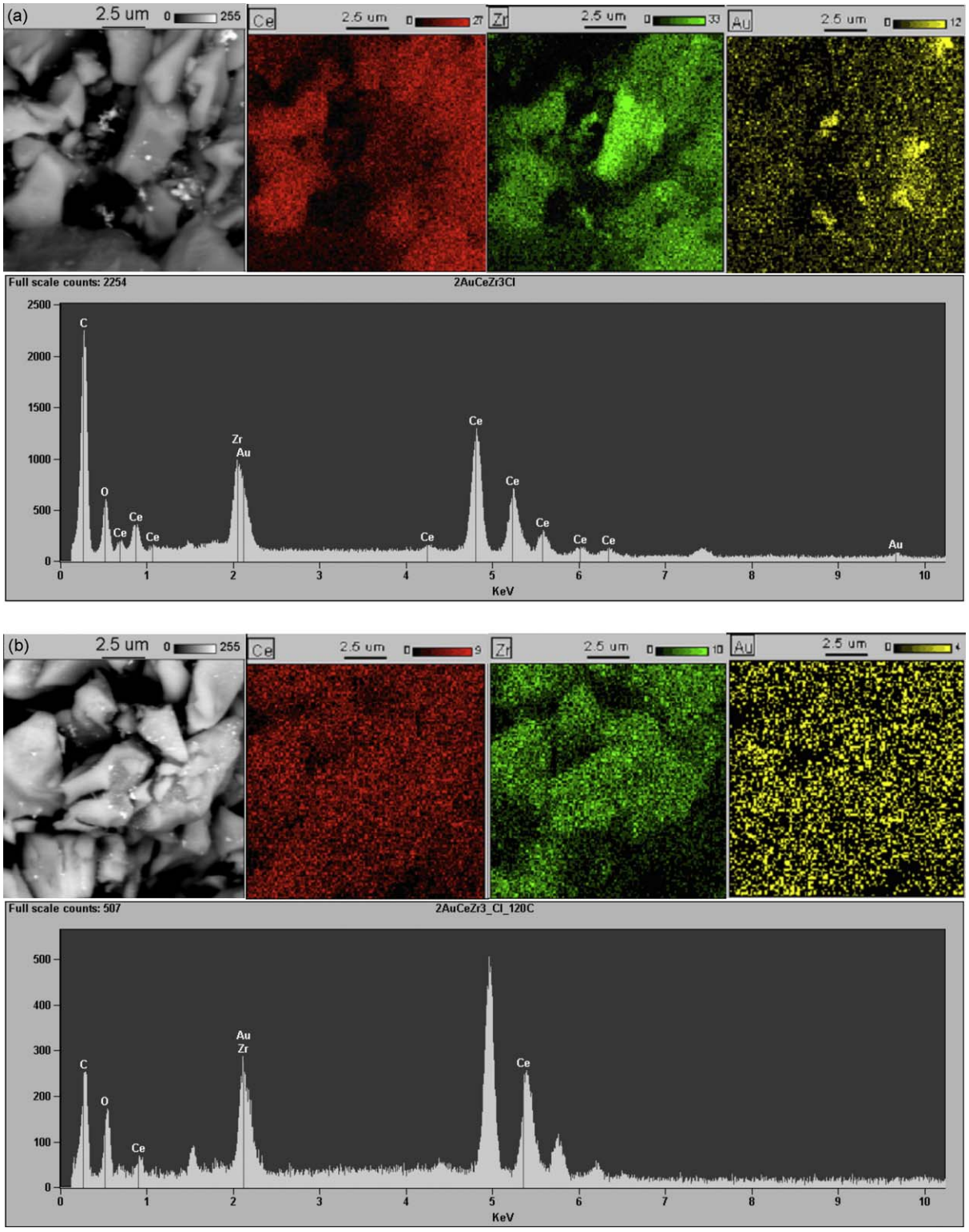

Fig. 1. The back-scattered electron (BSE) photomicrographs, EDS maps and characteristic X-ray spectra of $2Au/Ce_{0.75}Zr_{0.25}O_2$ catalysts prepared without washing: (a) calcined at 300 °C; (b) dried at 120 °C.

were found. In comparison to the catalysts prepared without washing and/or washed with warm water, one can observe that the application of ammonia as a washing agent strongly improves Au dispersion on the support surface. Moreover, the signal characteristic of Cl^- in the X-ray spectra is not visible (Fig. 2b).

Independent of the preparation procedure, a single cubic phase, fluorite-type structure of ceria was observed in $2Au/CeO_2$ catalysts. In the case of $2Au/CeO_2$–ZrO_2, prepared either without washing or washed with warm water/ammonia, at high CeO_2 concentration (75% mol) in the support, the cubic phase was favoured, whereas both for intermediate (50% mol) and ZrO_2-rich (75% mol) compo-

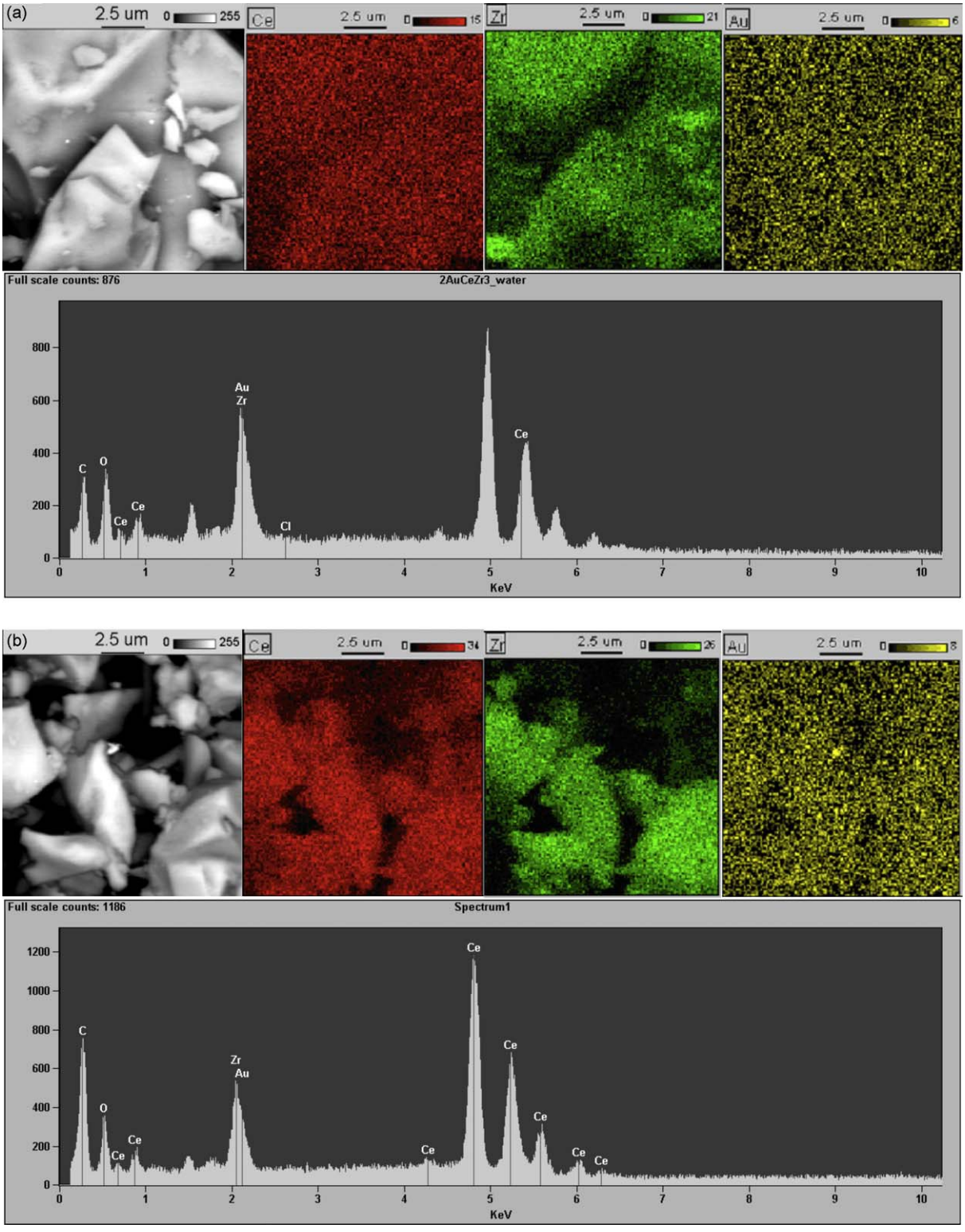

Fig. 2. The back-scattered electron (BSE) photomicrographs, EDS maps and characteristic X-ray spectra of $2Au/Ce_{0.75}Zr_{0.25}O_2$ catalysts: (a) washed with warm water; (b) washed with ammonia and calcined at 300 °C.

sition, tetragonal one is preferential, similarly to the oxide supports. Monoclinic and tetragonal phases of ZrO_2 were observed in $2Au/ZrO_2$ catalyst both unwashed and washed with both warm water and ammonia. In general, neither deposition of Au nor the washing treatment of the catalysts significantly influences crystallite size of the oxide supports (Table 1). Only in the case of $2Au/CeO_2$ catalyst washed with ammonia, the crystallite size of CeO_2 is twice lower than that estimated for the sample prepared excluding this preparation stage. In the case of $2Au/CeO_2$ and $2Au/CeO_2$–ZrO_2 catalysts washed with ammonia, a shift of the four main diffraction peaks, corresponding to both the (1 1 1) (2 2 0) (3 1 1) (2 0 0) reflections typical of a face-centered cubic (fcc) of ceria cell and the

(1 0 1) (1 1 0) (2 0 0) (2 1 1) reflections typical of a tetragonal cell, towards lower 2θ angles was observed. It could be related to the lattice expansion due to the formation of Ce^{3+} cations, having a bigger radius than Ce^{4+} (1.14 Å vs. 0.97 Å), suggesting the autoreduction of the catalysts surface in the presence of well-dispersed Au during the calcination process, as we proposed previously [17].

HRTEM technique was used for the selected, most representative samples, in order to determine an average Au particle size and to define their distribution more accurate. The mean Au particle diameters were calculated and are presented in Table 1. For the catalysts prepared without washing, irrespective of the oxide used as a support, a non-homogenous distribution of smoothed, mostly spherical or slightly elongated Au particles was found (Fig. 3a). For Au supported on CeO_2 and $Ce_{0.75}Zr_{0.25}O_2$, the majority of Au particles are in the range of 5–30 nm, whereas for $2Au/ZrO_2$ it ranges from 10 to 35 nm. Moreover, zirconium-supported catalyst presents broader Au particle size distribution. The formation of the large Au agglomerates is enhanced by both low specific surface area of ZrO_2 and sintering of Au particles, related to chloride residue.

The application of warm water as a washing agent leads to the decrease in the Au particle size. For $2Au/CeO_2$ and $2Au/Ce_{0.75}Zr_{0.25}O_2$, the majority of Au particles are in the range of 5–15 nm, and those supported on ZrO_2 are in the range of 5–20 nm. In spite of washing, the Au particles larger than 20 nm were also found. It could be related to the fact that the application of this type of washing procedure does not eliminate completely the residual chlorine from the catalysts [23]. The amount of residual chloride in Au/CeO_2 catalyst was found to be three times higher than that observed for zirconium-supported one, probably as a result of a different mechanism of chloride ions incorporation into the catalysts. Beside its presence in the exchanged Au species, the chloride ions from the metal precursor can also be incorporated into the ceria lattice either by occupation of an oxygen vacancy (Lewis type sites) or by an exchange of the support OH^- groups (Brönsted type sites), as reported by Force et al. [25]. Such an additional participation of Cl^- in the anionic exchange mechanism could be a reason of the higher amount of residual chlorine in the ceria-supported catalysts. It also implies that a lower dispersion of Au on ZrO_2 oxide is mostly related to a lower specific surface area of the support. Washing of the catalysts with ammonia significantly improves Au dispersion on the support surface (Fig. 3b). The presence of spherical Au particles of different size is observed. Majority of the Au particles supported on CeO_2 and $Ce_{0.75}Zr_{0.25}O_2$ are in the range of 1–5 nm, whereas for $2Au/ZrO_2$ it ranges from 1 to 7 nm. In spite of washing, the Au particles larger than 7 nm are present, especially for $2Au/ZrO_2$. As it could be seen, the application of ammonia as a washing agent successfully prevents the agglomeration of Au particles.

3.2. Surface composition

The effect of washing treatment on the surface composition of $Au/Ce_{1-x}Zr_xO_2$ catalysts was investigated by ToF-SIMS method. The representative surface images of CeO_2, $Ce_{0.75}Zr_{0.25}O_2$ and ZrO_2-based Au catalysts prepared without washing and washed with ammonia together with the corresponding negative-ion mode SIMS spectra are presented in Fig. 4. A series of ion clusters related to gold were found. The peak with m/z of 197 was assigned to Au^-. The peaks with m/z of 232, 248, and 267 were ascribed to ion fragments $AuCl^-$, $AuClO^-$, and $AuCl_2^-$, respectively. It confirms the presence of chloride ions in the surrounding of gold centres ($AuCl^-$, $AuCl_2^-$, etc.) at the catalysts surface. The intensity ratio of chloride ions to the total number of ions (Cl^-/total$^-$) is two to five times higher for the catalysts prepared without washing than for those washed with ammonia, depending on the oxide support (Table 2). For the catalysts prepared without washing the average Au particle size was also much higher (Table 1). It confirms the role of residual chlorine in the sintering of Au on the support surface. Interestingly, for the catalysts prepared without washing, the Cl^-/total$^-$ intensity ratio is higher for Au supported on Ce-containing oxides. It suggests higher affinity of ceria to chlorine, as proposed above. The values of the Cl^-/total$^-$ intensity ratios after washing with ammonia are similar for all studied catalysts. The presence of chloride ions is important in conjunction with their location. The $AuCl^-/Au^-$ and $AuCl_2^-/Au^-$ intensity ratios give information about the amount of Au bonded to or surrounded by chloride ions. It should be noted that those intensity ratios are also higher for the catalysts prepared without washing than for those washed with ammonia, especially in the case of Au/CeO_2. Moreover, in the case of the catalysts prepared without washing, the values of $AuCl^-/Au^-$, $AuCl_2^-/Au^-$ and $AuClO^-/Au^-$ intensity ratios are very high for Au/CeO_2 and $Au/Ce_{0.75}Zr_{0.25}O_2$ catalysts, whereas are low for $2Au/ZrO_2$ one. In ToF-SIMS spectra, the peaks with m/z of 213, 214, and 229 were also found and assigned to ion fragments AuO^-, $AuOH^-$, and AuO_2^-, respectively. It confirms the presence of oxygen ions in the surrounding of gold centres (AuO^-, AuO_2^-, etc.) at the catalysts surface. The AuO^-/Au^- and AuO_2^-/Au^- intensity ratios give information about the amount of Au bonded to or surrounded by oxygen ions (Table 2). It should be noted that those intensity ratios are several times higher for the catalysts prepared without washing than for those washed with ammonia. Moreover, for all studied catalysts, the AuO^-/Au^- intensity ratio is higher for Au supported on Ce-containing oxides.

Similarly to our results, a series of different ion clusters related to gold were also found over $Au/\gamma\text{-}Al_2O_3$ and Au/TiO_2 catalysts, as reported by Fu et al. [26]. For comparison, those authors also investigated a gold foil, yielding only the characteristic peaks of gold (m/z = 197) and $AuCl^-$ ion fragments (m/z = 232). However, the peaks associated with AuO^- $AuOH^-$, and AuO^{2-}, with m/z 213, 214, and 229, respectively, were not found. It let them to conclude that the peaks associated with AuO^- $AuOH^-$, and AuO_2^- result from fragmentation of particles on the surface, rather than recombination of species after ejection from the surface. It gave a direct evidence for the existence of oxidized gold on the studied catalysts surface. The same authors also used the XPS method to define the chemical structure of Au. Contrary to the ToF-SIMS results, only metallic Au was detected by XPS. This indicates that the amount of oxidized Au was too small to be detected by XPS, whereas ToF-SIMS, which is characterized with significantly higher sensitivity, made it possible. Considering the results reported by Fu et al. [26], it could be suggested that the presence of AuO^-, AuO_2^- and $AuOH^-$ ion clusters in SIMS spectra of studied $Au/Ce_{1-x}Zr_xO_2$ catalysts indicate the existence of oxidized gold in the catalysts, suggesting oxygen chemisorption on gold nanoparticles or partial oxidation of Au. Moreover, the presence of $AuOH^-$ ion clusters probably results from water chemisorbed on Au, as previously proposed [26]. Summarizing, it is important to note that the surface composition of the studied $Au/Ce_{1-x}Zr_xO_2$ catalysts strongly depends on both the preparation procedure and the oxide support (Table 2).

3.3. Reducibility characterization

CO was used as a reductant in our TPR investigations. The choice of this reducing agent, which is one of the reactant of the studied reaction, seems to be more adequate than using the most often applied in TPR studies hydrogen. TPR-CO measurements show a marked effect of Au particles on the reducibility of $Ce_{1-x}Zr_xO_2$

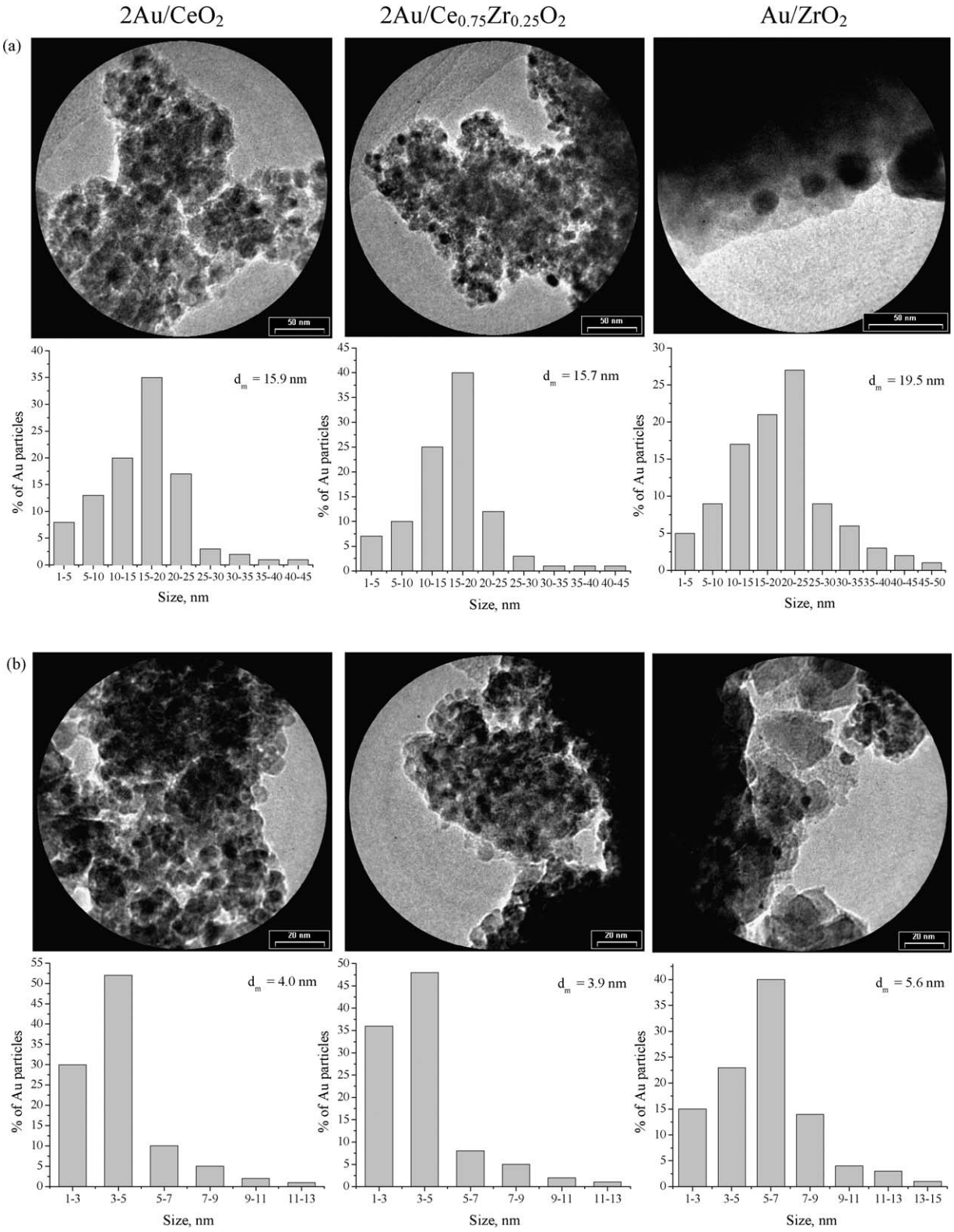

Fig. 3. The representative TEM images and the histograms of Au particle size distribution of Au catalysts supported on CeO_2, $Ce_{0.75}Zr_{0.25}O_2$ and ZrO_2: (a) prepared without washing; (b) washed with ammonia.

oxide supports. The detailed discussion of $Ce_{1-x}Zr_xO_2$ reducibility was presented in our previous paper [17]. Fig. 5a shows the TPR-CO profiles of $2Au/Ce_{1-x}Zr_xO_2$ catalysts prepared without washing. The low-temperature reduction peak of both $2Au/CeO_2$ and $2Au/CeO_2$–ZrO_2 catalysts consists of two overlapping peaks (Peaks I and II, Table 3). However, both shape and position of the peak present at a high temperature (Peak III, Table 3) remain almost unchanged, comparing to the corresponding oxide supports. In the TPR-CO profiles of both CeO_2 and Ce–Zr mixed oxides, beside the low-temperature reduction peak (260–650 °C), a characteristic

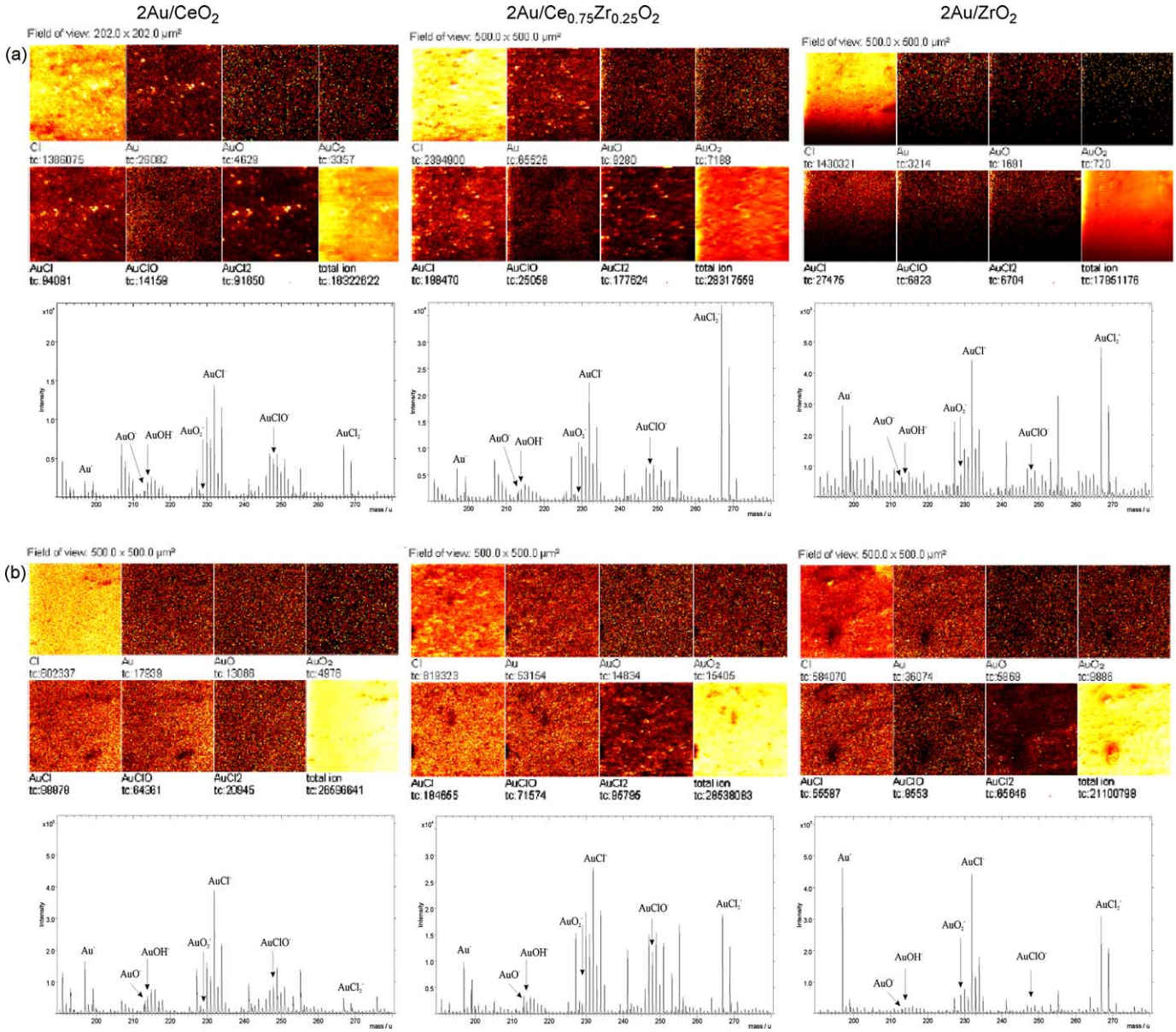

Fig. 4. The representative ToF-SIMS high-resolution images (bright colour indicates the investigated ions) and the corresponding mass spectrum of negative secondary ions of Au catalysts supported on CeO_2, $Ce_{0.75}Zr_{0.25}O_2$ and ZrO_2: (a) prepared without washing; (b) washed with ammonia.

shoulder in the temperature range 310–400 °C, depending on Ce/Zr molar ratio was observed [17]. This was related to the formation of intermediate phases as the origin of the low-temperature peak of CeO_2 reduction. Considering both a non-homogenous dispersion of Au on the catalysts prepared without washing and the existence of different intermediate phases of CeO_2, we suppose that the formation of CO_2 during the reduction of those catalysts at lower temperature occurs due to two processes. The first one (in the temperature range 200–450 °C) could be related to the reduction of both the oxygen species coordinated around finely dispersed gold particles and the surface capping oxygen of support, strongly anchored with Au. The presence of different gold-oxygen ion clusters was proposed basing on ToF-SIMS results (Fig. 4, Table 2). The second one (in the temperature range 430–650 °C) could be related to the reduction of both the oxygen species coordinated around larger gold agglomerates and the support surface layers being not strongly anchored with Au and/or unaffected by Au due to its non-uniform distribution, as confirmed by SEM–EDS (Fig. 1a) and HRTEM studies (Table 1). The TPR-CO profile of $2Au/ZrO_2$ catalyst consists of one peak with the maximum at 850 °C. Thus, this catalyst is much more resistant to the reduction, comparing to both $2Au/CeO_2$ and $2Au/CeO_2$–ZrO_2 systems. The temperature range at which the catalysts reduction occurs is similar to that of the oxide supports. However, for $2Au/CeO_2$–ZrO_2 catalysts the formation of CO_2 starts at a lower temperature than for $2Au/CeO_2$.

The quantity of CO_2 formed during the catalysts reduction, estimated on the basis of TPR-CO profiles, is lower ca. 10% than that observed for Ce–Zr mixed oxides. The detailed reducibility data for the corresponding oxide supports were presented in our previous paper [17]. The observed effect is more pronounced for Au supported on pure ceria (ca. 20%). In the case of $2Au/ZrO_2$, the total formation of CO_2 is only slightly lower than that observed for unsupported ZrO_2. As reported by Trovarelli [27], the residual anionic species (e.g., chlorides from the metal precursor) may significantly affect the reductive properties of supported metals such as Pt, Pd, Rh. Chloride may substitute oxygen ions in the ceria

Table 2
The values of selected secondary ions intensity ratios for some $2Au/Ce_{1-x}Zr_xO_2$ catalysts.

Intensity ratio	Catalyst denotation (the first number corresponds to the nominal wt.% content of Au)		
	$2Au/CeO_2$	$2Au/Ce_{0.75}Zr_{0.25}O_2$	$2Au/ZrO_2$
Without washing			
$Cl^-/total^-$	5.8×10^{-2}	5.6×10^{-2}	2.8×10^{-2}
AuO^-/Au^-	6.0×10^{-1}	4.2×10^{-1}	3.5×10^{-1}
$AuOH^-/Au^-$	1.2	5.4×10^{-1}	2.1×10^{-1}
AuO_2^-/Au^-	3.5×10^{-1}	2.7×10^{-1}	3.7×10^{-1}
$AuCl^-/Au^-$	9.8	4.2	1.5
$AuClO^-/Au^-$	3.1	1.2	3.2×10^{-1}
$AuCl_2^-/Au^-$	4.0	6.6	1.7
Washed with ammonia			
$Cl^-/total^-$	1.1×10^{-2}	1.5×10^{-2}	1.3×10^{-2}
AuO^-/Au^-	2.1×10^{-1}	2.2×10^{-1}	4.6×10^{-2}
$AuOH^-/Au^-$	3.7×10^{-1}	3.2×10^{-1}	4.8×10^{-2}
AuO_2^-/Au^-	2.6×10^{-1}	9.4×10^{-2}	1.4×10^{-1}
$AuCl^-/Au^-$	3.1	3.7	1.0
$AuClO^-/Au^-$	6.3×10^{-1}	1.3	5.2×10^{-2}
$AuCl_2^-/Au^-$	3.5×10^{-1}	1.9	6.4×10^{-1}

lattice during the reduction process. Le Normand et al. [28] have confirmed with XRD and XPS studies that CeO_2 surface can react with chlorine to form CeOCl or $Ce(OH)_2Cl$ phases in Pd/CeAl catalyst. Also, the presence of CeOCl phase was evidenced by XRD in Pd/CeO_2 catalysts by Kępinski et al. [29]. As we reported previously for Au/Mg_4Al_2 [3], some quantity of chloride introduced into the catalysts with Au precursor remains in the sample, even after the oxidative treatment. However, the amount of residual chlorine in the catalyst seems to be dependant on the kind of the oxide used as a support for Au. According to ToF-SIMS results, the value of $Cl^-/total^-$ ions intensity ratio in $2Au/CeO_2$ catalysts was two times higher than that observed in $2Au/ZrO_2$ one (Table 2). It suggests that the decrease in the amount of CO_2 formed during the catalysts reduction, comparing to the corresponding oxide supports, can be related to the presence of residual chlorine, probably resulting in the formation of CeOCl, which enhances the cerium stability in a low oxidation state. To support such a hypothesis, the effect of the residual chlorine on the reducibility of the unsupported oxide was investigated. The $Ce_{0.5}Zr_{0.5}O_2$ oxide was impregnated with chloride ions using HCl solution (9×10^{-4} M), as in the case of catalysts preparation (temperature, time of stirring, etc.). Similarly to the Au-containing catalysts, the obtained samples were dried and next calcined at 300 °C for 4 h. In the presence of chloride, the reducibility features like relative intensity and position of reduction peak of $Ce_{0.5}Zr_{0.5}O_2$ are different: the peak with the maximum at 500 °C becomes more intense, sharper and shifted towards higher temperature (520 °C) (Fig. 5b). The reduction of Cl^--containing $Ce_{0.5}Zr_{0.5}O_2$ oxide starts at temperature above 380 °C. This temperature is much higher than that observed for Cl^--free $Ce_{0.5}Zr_{0.5}O_2$ oxide (T_0, the initial reduction temperature, ca. 300 °C) (Fig. 5b). Based on Fig. 5b, it could be seen that the reduction of $2Au/Ce_{0.5}Zr_{0.5}O_2$ catalyst occurs in two stages with the maxima at 380 °C (Peak I) which can be ascribed to the reduction of both the oxygen species coordinated around finely dispersed gold particles and the surface capping oxygen of support, strongly anchored with Au, and at 520 °C (Peak II) reflecting the reduction of both the oxygen species coordinated around larger gold agglomerates and the chlorinated support surface layers being not strongly anchored with Au. Moreover, the quantity of CO_2 formed during the reduction of $Ce_{0.5}Zr_{0.5}O_2$ containing residual chlorine is lower than that for the chloride-free sample, corresponding to the reduction degree of 54.9% (0.93 mmol g^{-1}), instead of 78.6% (1.33 mmol g^{-1}), respectively. It confirms that the presence of chloride may significantly affect the reductive properties of the studied catalysts, stabilizing cerium in a low oxidation state.

The effect of washing with warm water on the TPR-CO profiles of $2Au/Ce_{1-x}Zr_xO_2$ catalysts is presented in Fig. 6a. At relatively low temperature, the TPR profile of $2Au/CeO_2$ and $2Au/CeO_2$–ZrO_2 catalysts consists of two overlapping peaks, similarly to the catalysts prepared without washing. However, washing with warm water affects the relative intensity, position and shape of those peaks. The peak present at 430 °C for $2Au/CeO_2$ prepared without washing becomes larger (Peak I) and on the other hand, that at 505 °C becomes smaller (Peak II). The significant shift of Peak I towards lower temperatures is observed. It should be reminded that the reduction of bulk oxygen ceria has been reported to occur at a temperature above 650 °C [17] and remains unchanged. A similar behaviour is observed for Au supported on Ce–Zr mixed oxides. According to TEM results, catalysts washed with warm water present higher Au dispersion and lower amount of Au particles agglomerations than those prepared without this preparation stage. It is observed that the contribution of the low-temperature part of the reduction peak (Peak I) increases with the increasing amount of finely dispersed Au particles on the catalyst surface. Considering presented statements it is possible to differentiate the reduction of the support surface strongly anchored with finely dispersed Au particles, occurring at lower temperature and the reduction of the support being in contact with larger gold agglomerates and/or unaffected by Au, occurring at higher temperature. The TPR-CO profile of $2Au/ZrO_2$ catalyst consists of one peak slightly shifted towards lower temperatures,

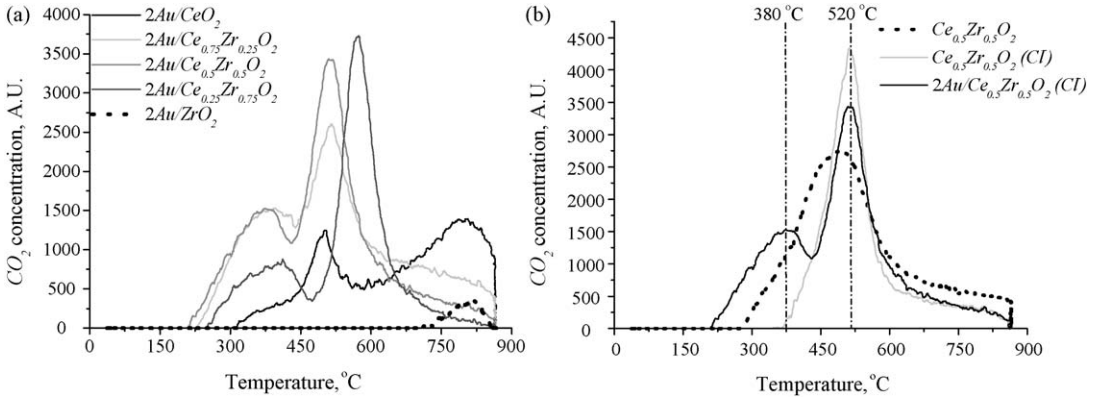

Fig. 5. TPR-CO profiles of: (a) $2Au/Ce_{1-x}Zr_xO_2$ catalysts prepared without washing; (b) $Ce_{0.5}Zr_{0.5}O_2$ "untreated" and Cl^--containing and $2Au/Ce_{0.5}Zr_{0.5}O_2$ catalyst prepared without washing.

Table 3
TPR-CO results of $2Au/Ce_{1-x}Zr_xO_2$ catalysts.

Sample denotation (the first number corresponds to the nominal wt.% content of Au)	Temperature (°C)				CO_2 formation (mmol g^{-1})
	T_0	Peak I	Peak II	Peak III	
Without washing					
$2Au/CeO_2$	315	430	505	840	0.81
$2Au/Ce_{0.75}Zr_{0.25}O_2$	235	400	520	780	1.24
$2Au/Ce_{0.5}Zr_{0.5}O_2$	215	380	520	760	1.18
$2Au/Ce_{0.25}Zr_{0.75}O_2$	255	420	575	–	0.79
$2Au/ZrO_2$	735	850	–	–	0.16
$Ce_{0.5}Zr_{0.5}O_2$	380	515	760	–	0.93
Washed with warm water					
$2Au/CeO_2$	280	380	520	840	0.79
$2Au/Ce_{0.75}Zr_{0.25}O_2$	195	320	530	760	1.06
$2Au/Ce_{0.5}Zr_{0.5}O_2$	175	290	500	740	1.02
$2Au/Ce_{0.25}Zr_{0.75}O_2$	215	410	570	–	0.71
$2Au/ZrO_2$	670	830	–	–	0.15
$Ce_{0.5}Zr_{0.5}O_2$	350	500	760	–	1.12
Washed with ammonia					
$2Au/CeO_2$	110	150	330	840	0.75
$2Au/Ce_{0.75}Zr_{0.25}O_2$	85	260	380	740	0.90
$2Au/Ce_{0.5}Zr_{0.5}O_2$	135	270	400	720	0.87
$2Au/Ce_{0.25}Zr_{0.75}O_2$	140	380	–	–	0.67
$2Au/ZrO_2$	670	820	–	–	0.14
$Ce_{0.5}Zr_{0.5}O_2$	330	500	760	–	1.31

T_0: the temperature at which the sample reduction starts (the initial reduction temperature). The reduction degrees of $Ce_{0.5}Zr_{0.5}O_2$ oxides by CO were calculated basing on the total quantity of CO_2 formed during the reduction process, according to the following equation: $Ce_{0.5}Zr_{0.5}O_2 + \delta CO \rightarrow Ce_{0.5}Zr_{0.5}O_{2-\delta} + \delta CO_2$, in details descried in Ref. [17].

compared with the catalyst prepared without washing. The most important difference among the analysed samples lies in the temperature at which the CO_2 formation starts as a result of catalysts reduction. For $2Au/CeO_2$–ZrO_2 catalysts, the reduction starts at significantly lower temperatures than that for $2Au/CeO_2$. However, no differences in the Au particle size distribution depending on the oxide used as a support are observed (Table 1). On the other hand, some quantities of residual chlorine were found in water-washed gold catalysts supported on both CeO_2 and ZrO_2 [23]. However, in the case of ceria-supported catalyst, the residual chlorine content was three times higher than that for ZrO_2-supported one. Considering the similar distribution of Au particles over different supports, we suppose that chlorine can react with CeO_2 surface to form CeOCl, inhibiting its reducibility, as discussed above. It results in a significantly higher reduction temperature in the case of Au/CeO_2 catalyst, comparing to Au supported on Ce–Zr mixed oxides. To sum up, it could be concluded that beside the dispersion of Au, the affinity of the support oxide to the residual chlorine affects the temperature at which the catalysts reduction occurs.

Although washing of the catalysts with warm water partially removes residual Cl^- ions, the quantity of CO_2 formed during their reduction, estimated on a basis of their TPR-CO profiles, is lower than that observed for the catalysts prepared without washing (Table 3). In order to check how the warm water treatment affects the reducibility of studied materials, $Ce_{0.5}Zr_{0.5}O_2$-mixed oxide containing residual chlorine was washed with warm water, under the same conditions as during the catalysts preparation. It reduction occurs in one stage with the maximum at 500 °C, similarly to the fresh one (Fig. 5b). Compared with the TPR-CO profile of Cl^--containing oxide (Fig. 5b), a decrease in the temperature and changes in the relative intensities of the observed reduction peaks were detected. The decrease in the relative intensity of Peak II (Fig. 6b vs. Fig. 5b), reflecting the reduction of both the oxygen species coordinated around larger gold agglomerates and the chlorinated support surface layers being not strongly anchored with Au was observed. Moreover, the increase in the relative intensity of Peak I (Fig. 6b vs. Fig. 5b) which can be ascribed to the reduction of both the oxygen species coordinated around finely dispersed gold particles and the surface capping

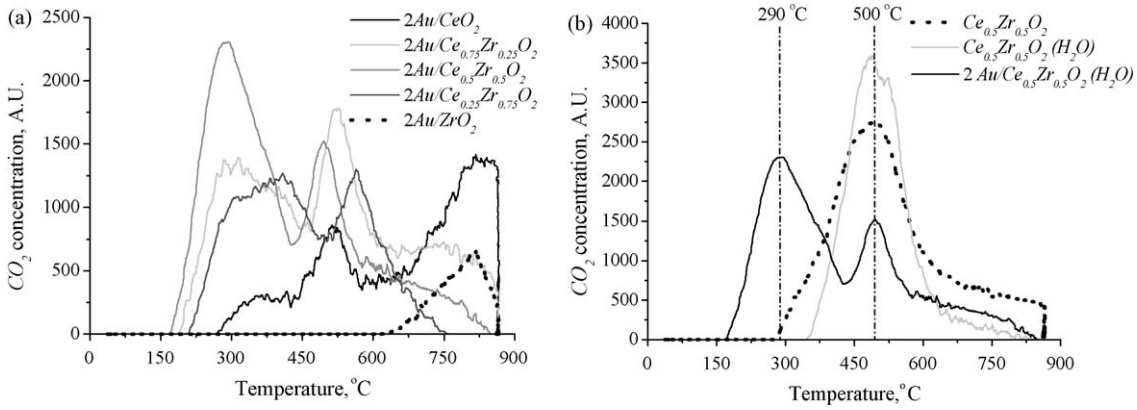

Fig. 6. TPR-CO profiles of: (a) $2Au/Ce_{1-x}Zr_xO_2$ catalysts washed with warm water; (b) $Ce_{0.5}Zr_{0.5}O_2$ "untreated" and washed with warm water and $2Au/Ce_{0.5}Zr_{0.5}O_2$ catalyst washed with warm water.

oxygen of support, strongly anchored with Au was noticed. It confirms that the application of warm water as a washing agent improves the dispersion of Au nanoparticles on the support surface. The observed shift of reduction Peaks (I and II) towards lower temperatures (Fig. 6b vs. Fig. 5b) proves that washing with warm water improves also the reducibility of the studied catalysts. However, the quantity of CO_2 formed during the reduction of "chlorinated and next washed with warm water" $Ce_{0.5}Zr_{0.5}O_2$ oxide is still lower than that estimated for the "untreated" one, corresponding to the reduction degree of 54.9% (1.12 mmol g^{-1}), instead of 78.6% (1.33 mmol g^{-1}), respectively. It could be related to the fact that the application of this type of washing procedure does not eliminate completely the residual chlorine from the catalysts [23]. It should be noted that the amount of CO_2 formed during the reduction of $2Au/Ce_{0.5}Zr_{0.5}O_2$ catalysts washed with warm water and dried at 120 °C is significantly lower (0.87 mmol g^{-1}) than that obtained for the same sample calcined at 300 °C (1.02 mmol g^{-1}). Moreover, those values are considerably lower than the amount of CO_2 formed during the reduction of "chlorinated and washed with warm water" $Ce_{0.5}Zr_{0.5}O_2$ oxide (1.12 mmol g^{-1}). It suggests the possibility of the partial reduction of the catalysts surface (catalysts autoreduction) during the temperature treatment. The autoreduction phenomenon is probably the reason of the change in the catalysts colour during drying and calcination processes from yellow to dark grey and from dark grey to graphite, respectively.

The effect of residual chlorine elimination with ammonia on the reducibility of the studied Au catalysts is shown in Fig. 7a. In the temperature range 25–500 °C two overlapping peaks are registered in the TPR-CO profiles of CeO_2, $Ce_{0.75}Zr_{0.25}O_2$ and $Ce_{0.5}Zr_{0.5}O_2$-based Au catalysts. Also, in the case of the oxide supports, beside the reduction peak a characteristic shoulder was observed at low temperature [17]. This suggests the existence of at least two types of Ce^{4+} located at different chemical environments, assigned to the reduction of surface and subsurface Ce^{4+} susceptible to the reduction at a lower temperature in the presence of well-dispersed Au. Moreover, at low temperature the reduction of oxygen species coordinated around finely dispersed Au particles can occur. The reduction peak present at a higher temperature, reflecting bulk reduction of CeO_2 accompanied by the formation of non-stoichiometric oxides of cerium remains almost unchanged. Similarly to $2Au/CeO_2$, the removal of residual chlorine with ammonia greatly improves the reducibility of $2Au/CeO_2$–ZrO_2 catalysts, comparing to those washed with warm water and/or prepared without washing. In the presence of homogenously dispersed gold nanoparticles, the reduction of surface oxygen of ceria–zirconia materials is effectively promoted and the characteristic shift of the low-temperature TPR-CO peak towards lower temperatures is observed. The reduction of $2Au/Ce_{0.25}Zr_{0.75}O_2$ occurs in one stage with the maximum at 380 °C, similarly to the $Ce_{0.25}Zr_{0.75}O_2$ oxide. However, the temperature range at which the catalysts reduction takes place is significantly lower. For $2Au/ZrO_2$ catalyst, the TPR-CO profile consists of one peak with the maximum at 820 °C.

As it could be seen, the reducibility of Ce-containing Au catalysts appears to be dependent on the amount of oxygen anions attached to surface Ce^{4+} ions and their preparation conditions. For ammonia washed catalysts, the surface capping oxygen reactivity (Peak I) is the highest due to the presence of highly dispersed Au particles. Such behaviour could be related to the adsorption of CO molecules on well-dispersed metallic gold particles and next to the migration by a spillover process from the Au particles on the support surface [17]. That process is favoured by a high dispersion of gold. However, if the catalyst contains only ionic gold, the surface oxygen reducibility could be intensified through the lattice substitution mechanism, as proposed by Fu et al. [30]. According to those statements, the Au^+ or Au^{3+} ions would fill the vacant Ce^{4+} sites resulting in the oxygen vacancies formation and the increase in oxygen mobility and reducibility. It results in a decrease in the strength of the surface Ce–O bonds adjacent to gold atoms and leads to higher surface lattice oxygen mobility [31].

In the case of $2Au/CeO_2$ catalyst washed with ammonia (Table 3) the amount of CO_2 formed during its reduction is lower ca. 25% than that observed for CeO_2 oxide (0.99 mmol g^{-1}) [17]. It is also lower than the quantity of CO_2 estimated for the catalysts both prepared without washing and washed with warm water (Table 3). This effect is even more pronounced for $2Au/CeO_2$–ZrO_2 oxides (ca. 35%). For $2Au/ZrO_2$, the total formation of CO_2 is only slightly lower than that observed for unsupported ZrO_2 (0.20 mmol g^{-1}). Moreover, the AuO^-/Au^- and AuO_2^-/Au^- intensity ratios, giving information about the amount of Au bonded to or surrounded by oxygen ions, were lower for the catalysts washed with ammonia. Considering that washing of the Au catalysts with ammonia allows to remove residual chlorine [3], which inhibits the reducibility of Ce-containing oxides, the possibility of catalysts autoreduction during the calcination step could be suggested. In order to check how ammonia treatment affects the reducibility of the studied materials, $Ce_{0.5}Zr_{0.5}O_2$ oxide containing residual chlorine was washed with ammonia, according to the same conditions as during the catalysts preparation. The reduction of $Ce_{0.5}Zr_{0.5}O_2$-mixed oxide washed with ammonia occurs in one stage with the maximum at 500 °C, similarly to the "untreated" one (Fig. 7b). Moreover, the quantity of CO_2 formed during the

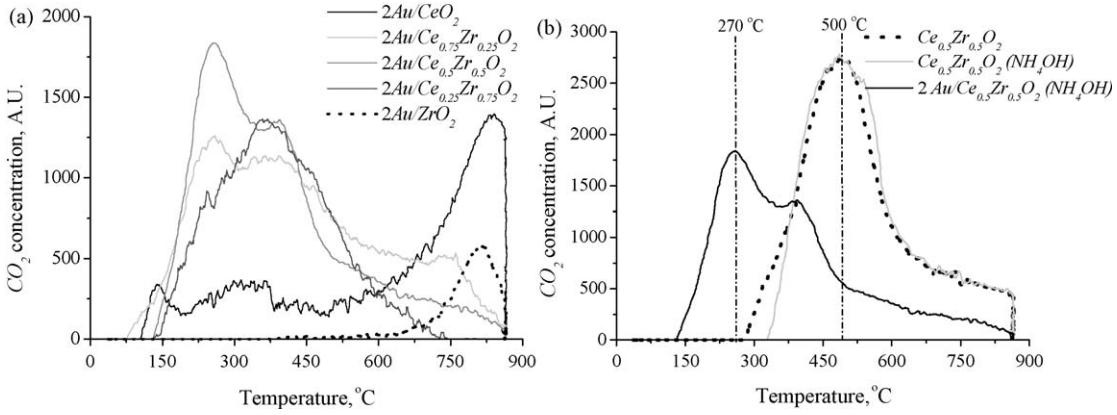

Fig. 7. TPR-CO profiles of: (a) $2Au/Ce_{1-x}Zr_xO_2$ washed with ammonia; (b) $Ce_{0.5}Zr_{0.5}O_2$ "untreated" and washed with ammonia and $2Au/Ce_{0.5}Zr_{0.5}O_2$ catalyst washed with ammonia.

reduction of "chlorinated and next washed with ammonia" $Ce_{0.5}Zr_{0.5}O_2$ oxide (1.31 mmol g^{-1}) is similar to that estimated for the "untreated" one (1.33 mmol g^{-1}), and corresponds to the reduction degree of 77.4% and 78.6%, respectively. This confirms that a lower amount of CO_2 created during the reduction of ammonia washed catalysts, compared with the oxide supports is related to a catalysts autoreduction phenomenon. It should be noted that the removal of residual Cl^- with ammonia from the studied materials prevents successfully both the agglomeration of Au particles and the changes in their reducibility. We suppose that chlorine can react with CeO_2 surface to form CeOCl, stabilizing cerium in a low oxidation state, and in the same way can inhibit its reductive properties.

Thus, washing of the catalysts both with warm water and ammonia leads to a decrease in the average Au particle size and improves its dispersion. The presence of highly dispersed Au promotes the reducibility of the surface oxygen of the oxide support of the studied catalysts at lower temperatures. Its effect on the catalysts activity in CO oxidation is discussed below.

3.4. Catalytic tests

The activity of $2Au/Ce_{1-x}Zr_xO_2$ catalysts in CO oxidation, synthesized by different preparation procedures is presented in Table 4. CO conversion increases with the increase in reaction temperature. The $2Au/Ce_{1-x}Zr_xO_2$ catalysts prepared without washing began to oxidize CO to CO_2 at around 170–220 °C. Their activity in CO oxidation was found to be dependent on Ce/Zr molar ratio of the oxide support, with a maximum obtained for $2Au/Ce_{0.5}Zr_{0.5}O_2$ (Ce/Zr molar ratio = 1). Total CO conversion below 300 °C was observed only in the case of Au supported on Ce–Zr mixed oxides. CO conversion over Au supported on both CeO_2 and ZrO_2 was very low: 50% or almost no conversion at 300 °C, respectively. All $2Au/Ce_{1-x}Zr_xO_2$ catalysts prepared without washing are characterized by similar Au content and its dispersion (Fig. 3, Table 1). However, the difference in their activity in CO oxidation is very well marked.

The catalysts washed with warm water were active at lower temperatures compared with those prepared without washing, with 100% CO conversion at 150 °C over $2Au/Ce_{0.5}Zr_{0.5}O_2$. Total CO conversion below 200 °C was observed only in the case of Au supported on Ce–Zr mixed oxides. A very low CO conversion over Au supported on either CeO_2 or ZrO_2 was detected: 85% or 9% at 300 °C, respectively. The observed increase in activity is related to the decrease in the Au particle size after washing the catalysts with warm water. Irrespective of the oxide used as a support, similar Au dispersion is observed (Fig. 3, Table 1). In the case of $2Au/ZrO_2$ catalysts, both much lower reducibility and Au dispersion are the reason of their poor activity. In the case of the catalysts washed with ammonia a very significant decrease in the temperature of 10% and 50% CO conversion was observed. The increase in activity is related to a significant decrease in the Au particle size. The highest activity was observed over $2Au/Ce_{0.75}Zr_{0.25}O_2$ catalyst (Table 4). Interestingly, the chloride ions in the surrounding of gold centres ($AuCl^-$, $AuCl_2^-$, etc.) are still present at the surface of the most active catalyst in CO oxidation, as confirmed by ToF-SIMS studies. It suggests that the physico-chemical properties and catalytic performance of $Au/Ce_{1-x}Zr_xO_2$ catalysts in CO oxidation depend also on the concentration of residual chlorine. Recently, the effect of the chloride amount on the catalytic activity of $Au(K)/Fe_2O_3$ catalyst was also observed by Jóźwiak et al. [32]. They presented that the impregnated catalyst with Cl/Au = 4 ratio shows considerable activity. However, the further increase in Cl/Au ratio above 8 led to catalyst deactivation.

As it could be seen, the application of different preparation procedures led to obtain the $2Au/Ce_{1-x}Zr_xO_2$ catalysts with the different catalytic activity in CO oxidation. The obtained results indicate that the presence of residual chlorine in the studied catalysts evidently influences the catalytic performance of $Ce_{1-x}Zr_xO_2$ supported Au catalysts for low-temperature CO oxidation. To sum up, the activity of the catalysts both prepared without washing and washed with warm water increases in the following order:

$$Au/ZrO_2 < Au/CeO_2 < Au/Ce_{0.25}Zr_{0.75}O_2 < Au/Ce_{0.75}Zr_{0.25}O_2 < Au/Ce_{0.5}Zr_{0.5}O_2.$$

The activity of catalysts washed with ammonia is dependent on Ce/Zr molar ratio in the oxide used as a support for Au, increasing in the following order:

$$Au/ZrO_2 < Au/Ce_{0.25}Zr_{0.75}O_2 \approx Au/Ce_{0.5}Zr_{0.5}O_2 < Au/CeO_2 < Au/Ce_{0.75}Zr_{0.25}O_2.$$

The application of each preparation procedure applied in this study leads to obtain the similar Au content and its dispersion over CeO_2 and Ce–Zr mixed oxides (Table 1). However, the differences in both the catalytic performance and the reducibility of each series of $Au/Ce_{1-x}Zr_xO_2$ catalysts in CO oxidation are very well marked. The presence of highly dispersed Au nanoparticles effectively promotes both the reduction of the catalysts surface and its catalytic activity at low temperature. The observed correlations confirm the effect of Au particle size on the support redox properties and its role in the creating of $Au/Ce_{1-x}Zr_xO_2$ catalytic activity. According to the literature [7–9], higher reducibility increases the concentration of surface oxygen vacancies in the stationary state of the reaction, which can be the centres of oxygen activation. Such vacancies may be formed even in the reaction mixture CO + O_2 exhibiting lower redox potential compared to the oxygen atmosphere, as proposed by Grzybowska-Świerkosz [10]. It should be noted that in the case of CeO_2 and Ce–Zr mixed oxide supports no CO conversion at temperatures below 200 °C was observed [17]. However, in the presence of well-dispersed Au their catalytic performance is greatly improved. As reported by Guzman et al. [33], the adsorption of CO on Au^{3+}, Au^+, and Au^0 species was observed in the case of Au/CeO_2 catalyst. Moreover, the presence of

Table 4
The activity of $2Au/Ce_{1-x}Zr_xO_2$ catalysts in CO oxidation.

Catalyst denotation (the first number corresponds to the nominal wt.% content of Au)	Temperature (°C)	
	T_{10} °C	T_{50} °C
Without washing		
$2Au/CeO_2$	230	295
$2Au/Ce_{0.75}Zr_{0.25}O_2$	185	245
$2Au/Ce_{0.5}Zr_{0.5}O_2$	165	230
$2Au/Ce_{0.25}Zr_{0.75}O_2$	220	270
$2Au/ZrO_2$	n.d.	n.d.
Washed with warm water		
$2Au/CeO_2$	190	245
$2Au/Ce_{0.75}Zr_{0.25}O_2$	90	135
$2Au/Ce_{0.5}Zr_{0.5}O_2$	85	125
$2Au/Ce_{0.25}Zr_{0.75}O_2$	110	155
$2Au/ZrO_2$	n.d	n.d
Washed with ammonia		
$2Au/CeO_2$	<20	50
$2Au/Ce_{0.75}Zr_{0.25}O_2$	<20	35
$2Au/Ce_{0.5}Zr_{0.5}O_2$	50	95
$2Au/Ce_{0.25}Zr_{0.75}O_2$	60	105
$2Au/ZrO_2$	160	230

T_{10}, T_{50}: the temperature for 10% and 50% CO conversion was obtained, respectively; n.d.: not detected in the temperature range 25–300 °C; ($CO:O_2:He$ = 1.7:3.4:94.9 - vol.%; W/F = 0.12 g s cm^{-3}).

an additional band assigned to Ce^{4+}–CO was found, which confirms CO adsorption on CeO_2. It suggests the synergetic effect between the support and gold particles at the interface, as we mentioned above. Most recently, the Au–ZnO interaction and its influence on the structure and activity of Au/ZnO/SiO2 in CO oxidation was reported by Qian et al. [34]. They demonstrated that the stronger Au–ZnO interactions and the finer supported Au nanoparticles, the higher catalytic activity.

The present study has demonstrated the effects of the preparation procedure and the physico-chemical properties of the oxide supports on the catalytic activity of $Au/Ce_{1-x}Zr_xO_2$ catalysts in CO oxidation. A special attention was paid to the correlations between structural, redox and catalytic properties of $Au/Ce_{1-x}Zr_xO_2$ systems. Table 5 presents a brief comparison of some representative activity data obtained in this work to those reported in the literature, taking into consideration different preparation techniques, morphology of oxide support, gold particle size, calcination temperature, experimental conditions, etc. The activity of Au/CeO_2 catalysts prepared by both so-called SCS [36] and deposition precipitation [37] methods, calcined at 500 and 400 °C, respectively, and tested under similar reaction conditions, is definitively lower than that reported in this paper. Moreover, those catalysts [36,37] exhibit bigger particle size of both Au and CeO_2. The studied Au/CeO_2 catalyst shows similar activity in CO oxidation in air at room temperature to the ceria-supported Au catalysts reported by Casaletto et al. [5] and Liotta et al. [38], at significantly lower amount of Au. Recently, Carrettin et al. [35], Pillai and Deevi [39] and Chang et al. [40] have presented exceptionally high activity of Au/CeO_2 synthesized by DP for CO oxidation in air. The observed Au nanoparticles had a mean diameter of approximately 4 nm, similarly to the catalyst reported in this paper. However, those catalysts were neither calcined nor pretreated in situ before reaction testing. According to Pillai and Deevi [39], the exposure of the catalyst to ambient air overnight after its thermal treatment at 100 °C enhances the catalyst activity for the oxidation reaction. It suggests that the observed high activity over Au/CeO_2 could be attributed to the beneficial effect of the adsorption of water molecules from the atmosphere by the catalyst. On the other hand, the higher amount of oxygen vacancies present in nanosized (4 nm) ceria support was responsible for the activation of oxygen over Au/CeO_2 catalyst during CO oxidation reaction, as reported by Carrettin et al. [35]. A similar bahaviour in CO oxidation was observed over different Au/ZrO_2 catalysts [43]. The continuous decrease in ZrO_2 support particle size not only led to the continuous increase in Au-oxide boundaries in the Au/ZrO_2 catalyst but also modified the chemical properties at such boundaries due to the presence of a larger number of oxygen vacancies at the surfaces of smaller ZrO_2 nanoparticles. Consider-

Table 5
Comparison of activity in CO oxidation over CeO_2, ZrO_2 and CeO_2–ZrO_2-supported Au catalysts.

Oxide support	Prep. method[a]	Treat. temp. (°C)	S_{BET}[b] ($m^2\ g^{-1}$)	Au loading (wt.%)	Au particle size[c] (nm)	Support crystalline structure[d]	Support particle size[d] (nm)	Reaction conditions; catalyst weight	Activity CO conv.[e] (%)	T_{50}[f] (°C)	Ref.
CeO_2	DP	100	180	2.8	4	Cubic (fluorite) monoclinic	4[c]	$CO/O_2/He/N_2$ = 0.8/0.4/40.4/58.4; W/F = 18.6 g h mol_{CO}^{-1}	100	n.r.	35
CeO_2	SCS	500	36.9	2.0	5–25	Cubic (fluorite)	n.r.	2300 ppm CO, 7% O_2, He balance, W/F = 0.12 g s cm^{-3}; 800 mg	0	272	36
CeO_2	CB	400	24	3.0	9[d]	Cubic (fluorite)	10	CO/O_2/He = 2/2/96 molar ratio, 50 $cm^3\ min^{-1}$; 20 mg	0	150	37
CeO_2	DP	300	79*	3.0	15[d]	Cubic (fluorite)	n.r.	1% CO, 1% O_2, He balance, 50 $cm^3\ min^{-1}$; 50 mg	20	47	5
CeO_2	CP	400	41	10.0	8[d]	Cubic (fluorite)	7	1.0% CO, 1% O_2, He balance, 50 $cm^3\ min^{-1}$; 50 mg	5	92	38
CeO_2	DP	110	32	1.0	2–5	Cubic (fluorite)	12	3.6% CO, 21% O_2, Ar balance, 1000 $cm^3\ min^{-1}$; 50 mg	100	n.r.	39
CeO_2	DP	120	n.r.	1.0	2–4	Cubic (fluorite)	8.6	1% CO, air balance, 50 $cm^3\ min^{-1}$; 60 mg	65	n.r.	40
CeO_2	DAE	300	51.5	1.79	4	Cubic (fluorite)	6.4	1.6% CO, 3.3% O_2, He balance, 50 $cm^3\ min^{-1}$; 100 mg	15	50	[g]
ZrO_2	DP	200	235*	2.6	2	Amorphous	n.r.	1% CO, air balance, 250 $cm^3\ min^{-1}$; 46 mg	n.r.	−18	41
ZrO_2	DP	300	235*	2.6	4–8	Amorphous	n.r.	1% CO, air balance, 250 $cm^3\ min^{-1}$; 46 mg	n.r.	50	41
ZrO_2	DP	400	153	3.0	4.1	Orthorhombic	n.r.	0.18% CO, air balance, 73 $cm^3\ min^{-1}$; 250 mg	65	5	42
ZrO_2	DP	400	55	0.71	4.7	Monoclinic tetragonal	10–15[av.]	1% CO, air balance, 20,400 $cm^3\ h^{-1}\ g_{cat}^{-1}$; 100 mg	n.r.	80	42
ZrO_2	DP	400	34	0.63	5.3	Monoclinic tetragonal	20–25[av.]	1% CO, air balance, 20,400 $cm^3\ h^{-1}\ g_{cat}^{-1}$; 100 mg	n.r.	90	43
ZrO_2	SCS	500	33.9	2.0	5–25	n.r.	n.r.	2.3% CO, 7% O_2, He balance, W/F = 0.12 g s cm^{-3}; 800 mg	0	242	36
ZrO_2	DAE	300	3.8	1.45	5.6	Monoclinic tetragonal	27.8 18.8	1.6% CO, 3.3% O_2, He balance, 50 $cm^3\ min^{-1}$; 100 mg	0	230	[g]
$Ce_{0.8}Zr_{0.2}O_2$	DP	300	n.r.	2.0	n.r.	Cubic (fluorite)	15.1	0.5 $cm^3\ min^{-1}$ CO, 33.3 $cm^3\ min^{-1}$ air; 50 mg	0	100	44
$Ce_{0.75}Zr_{0.25}O_2$	DAE	300	49.5	1.68	3.9	Cubic (fluorite)	7.2	1.6% CO, 3.3% O_2, He balance, 50 $cm^3\ min^{-1}$; 100 mg	35	35	[g]

n.r. Not reported; *, data obtained for unsupported oxide.
[a] Abbreviations used: DP, deposition–precipitation; SCS, combustion synthesis; CB, combustion; CP, co-precipitation; DAE, direct anionic exchange.
[b] N_2 adsorption.
[c] Determined by TEM.
[d] Determined by XRD.
[e] CO conversion obtained at room temperature.
[f] Temperature at which 50% CO conversion was obtained.
[g] Present work.

Table 6
The summary of the correlations between structural, redox and catalytic properties of $2Au/Ce_{1-x}Zr_xO_2$ catalysts.

Sample denotation (the first number corresponds to the nominal wt.% content of Au)	Surface area[a] ($m^2\ g^{-1}$)	Au particle size[b] (nm)	Crystallite structure[c]	T_0[d]	Cl^-/total[e]	$AuCl^-/Au^-$[e]	AuO^-/Au^-[e]	T_{10} (°C)[f]	T_{50} (°C)[f]
Without washing									
$2Au/CeO_2$	50.0	15.9	Cubic	315	5.8×10^{-2}	9.8	6.0×10^{-1}	230	295
$2Au/Ce_{0.75}Zr_{0.25}O_2$	46.5	15.7	Cubic	235	5.6×10^{-2}	4.2	4.2×10^{-1}	285	245
$2Au/ZrO_2$	2.8	19.5	Monoclinic tetragonal	735	2.8×10^{-2}	1.5	3.5×10^{-1}	n.d	n.d
Washed with ammonia									
$2Au/CeO_2$	51.5	4.0	Cubic	110	1.1×10^{-2}	3.1	2.1×10^{-1}	<20	50
$2Au/Ce_{0.75}Zr_{0.25}O_2$	49.5	3.9	Cubic	85	1.5×10^{-2}	3.7	2.2×10^{-1}	<20	35
$2Au/ZrO_2$	3.8	5.6	Monoclinic tetragonal	670	1.3×10^{-2}	1.0	4.6×10^{-2}	160	230

T_{10}, T_{50}: The temperature for 10% and 50% CO conversion was obtained, respectively; n.d.: not detected in the temperature range 25–300 °C; T_0: temperature at which the sample reduction starts (initial reduction temperature).
[a] Determined by N_2-BET.
[b] Determined by HRTEM.
[c] Determined by XRD.
[d] Determined by TPR-CO.
[e] Determined by ToF-SIMS.
[f] Determined by CO oxidation ($CO:O_2$:He = 1.7:3.4:94.9 vol.%; W/F = 0.12 g s cm^{-3}).

ing catalysts characterized with similar ZrO_2 particles size, it could be seen that the temperature of 50% CO conversion reported by Zhang et al. [43] is lower than that obtained by us. However, the O_2/CO ratio used in their catalytic tests (O_2/CO = 21) was much higher than that of our experiments (O_2/CO = 2). The surface area of ZrO_2 support was also much higher, suggesting the existence of many factors influencing the activity of Au/oxide systems in CO oxidation. On the other hand, the temperature of 50% CO conversion over Au/ZrO_2 catalyst synthesized by so-called SCS method [36] is comparable with the data obtained in our paper. The application of dissimilar reaction conditions generates different activities over Au/ZrO_2 catalysts as reported by Wolf and Schüth [41] and Konova et al. [42]. The temperature of 50% CO conversion observed for $Au/Ce_{0.75}Zr_{0.25}O_2$ catalyst washed with ammonia is much lower than that of the most active system employed in Ref. [44]. Since both CO/O_2 molar ratio and Au loading are higher and simultaneously the activity of the catalyst synthesized by Wang et al. [44] is lower, the physico-chemical properties of oxide support, among them its particle size, appear to be very important. Therefore, the decrease in particle size of both Au and support oxide can lead to the increase in activity of Au/oxide systems in CO oxidation. It suggests that the modifications of the structural and redox properties of support can turn it in material adequate for the preparation of highly active catalysts.

4. Conclusions

The correlations between structural, redox and catalytic properties of $Au/Ce_{1-x}Zr_xO_2$ catalysts prepared using different synthesis procedures have been studied and are summarized in Table 6. The following main conclusions can be drawn:

- The poisoning effect of residual chlorine on the catalytic activity of $Au/Ce_{1-x}Zr_xO_2$ catalysts in CO oxidation was confirmed. One can observe the agglomeration of Au particles during the calcination step in the presence of residual chlorine. Chlorine removal during the washing treatment inhibits the sintering process and leads to the increase in activity of the studied systems. The series of catalysts washed with ammonia shows both the highest activity and smallest Au nanoparticles.
- The dispersion of Au is not the only one parameter determining the reactivity of $Au/Ce_{1-x}Zr_xO_2$ catalysts in CO oxidation. The physico-chemical properties of oxide support, among them its particle size, appear to be very important. The observed increase in activity is also related to higher oxygen mobility at lower temperature observed for Au nanoparticles supported on fluorite-structured oxides and the lower reduction temperature of Ce^{4+}, as determined by TPR-CO measurements.
- The sequence of increasing activity is followed by the sequence of increasing reducibility of the catalysts. This indicates the importance of the support redox properties in the creation of the catalytic performance of Au/oxide support contacts.
- The observed correlation between activity in CO oxidation and reducibility confirms that oxygen vacancies on the support surface are centers for oxygen molecule activation in this reaction.

Acknowledgements

This research was supported by Grant PBZ-KBN-116/T09/2004 (No. K124/1B/2005). The authors are grateful to Dr. J. Grams for performing ToF-SIMS measurements and to Dr. Miguel Ángel Gómez García for fruitful discussions.

References

[1] G.C. Bond, D.T. Thompson, Catal. Rev.-Sci. Eng. 41 (3–4) (1999) 319–388.
[2] A.S.K. Hashmi, G.J. Hutchings, Angew. Chem. Int. Ed. 45 (2006) 7896–7937.
[3] I. Dobrosz, K. Jiratova, V. Pitchon, J.M. Rynkowski, J. Mol. Catal. A: Chem. 234 (2005) 187–197.
[4] E.D. Park, J.S. Lee, J. Catal. 186 (1999) 1–11.
[5] M.P. Casaletto, A. Longo, A.M. Venezia, A. Martorana, A. Prestianni, Appl. Catal. A: Gen. 302 (2006) 309–316.
[6] Z. Ma, S.H. Overbury, S. Dai, J. Mol. Catal. A: Chem. 273 (2007) 186–197.
[7] H. Liu, A.I. Kozlov, A.P. Kozlova, T. Shida, K. Asakura, Y. Iwasawa, J. Catal. 185 (1999) 252–264.
[8] D. Horvath, L. Toth, L. Guczi, Catal. Lett. 67 (2000) 117–128.
[9] M.M. Schubert, S. Hackenberg, A.C. van Veen, M. Muhler, V. Plzak, R.J. Behm, J. Catal. 197 (2001) 113–122.
[10] B. Grzybowska-Świerkosz, Catal. Today 112 (2006) 3–7.
[11] J.-D. Grunwaldt, A. Baiker, J. Phys. Chem. 103 (1999) 1002–1012.
[12] H.-S. Oh, J.H. Yang, C.K. Costello, Y.M. Wang, S.R. Bare, H.H. Kung, M.C. Kung, J. Catal. 210 (2002) 375–386.
[13] A. Schulz, M. Hargittai, Chem. Eur. J. 7 (2001) 3657–3670.
[14] H.H. Kung, M.C. Kung, C.K. Costello, J. Catal. 216 (2003) 425–432.
[15] B. Qiao, Y. Deng, Appl. Catal. B: Environ. 66 (2006) 241–248.
[16] I. Sobczak, A. Kusior, J. Grams, M. Ziolek, J. Catal. 245 (2007) 259–266.
[17] I. Dobrosz-Gómez, I. Kocemba, J.M. Rynkowski, Appl. Catal. B: Environ. 83 (2008) 240–255.
[18] S. Ivanova, C. Petit, V. Pitchon, Appl. Catal. A: Gen. 267 (2004) 191–201.
[19] I. Dobrosz, I. Kocemba, J.M. Rynkowski, Pol. J. Environ. Stud. 15 No. 6A (2006) 32–36.

[20] J. Grams, J. Góralski, T. Paryjczak, Surf. Sci. Lett. 549 (2004) L21–L26.
[21] I. Dobrosz, M.A. Gómez-García, I. Kocemba, W. Maniukiewicz, J.M. Rynkowski, Pol. J. Environ. Stud. 14 (IV) (2005) 231–234.
[22] S. Ivanova, V. Pitchon, Y. Zimmermann, C. Petit, Appl. Catal. A: Gen. 298 (2006) 57–64.
[23] S. Ivanova, V. Pitchon, C. Petit, J. Mol. Catal. A: Chem. 256 (2006) 278–283.
[24] J. Soria, J.C. Conesa, A. Martýnez-Arias, Colloid Surf. A: Phys. Eng. Aspect. 158 (1999) 67–74.
[25] C. Force, J.P. Belzunegui, J. Sanz, A. Martinez-Arias, J. Soria, J. Catal. 197 (2001) 192–199.
[26] L. Fu, N.Q. Wu, J.H. Yang, F. Qu, D.L. Johnson, M.C. Kung, H.H. Kung, V.P. Dravid, J. Phys. Chem. Lett. B 109 (2005) 3704–3706.
[27] A. Trovarelli (Ed.), ICP (2002) 15–50.
[28] F. Le Normand, L. Hilaire, K. Kili, G. Grill, G. Maire, J. Phys. Chem. 92 (1988) 2561–2568.
[29] L. Kępinski, M. Wolcyrz, J. Okal, J. Chem. Soc., Faraday Trans. 91 (1995) 507–515.
[30] Q. Fu, H. Saltsburg, M. Flytzani-Stephanopoulos, Science 301 (2003) 935–938.
[31] S. Scirè, M. Minicò, C. Crisafulli, C. Satriano, A. Pistone, Appl. Catal. B: Environ. 40 (2003) 43–49.
[32] W.K. Jóźwiak, E. Kaczmarek, W. Ignaczak, Pol. J. Environ. Stud. 14 (2005) 127–130.
[33] J. Guzman, S. Carrettin, A. Corma, J. Am. Chem. Soc. 127 (2005) 3286–3287.
[34] K. Qian, W. Huang, J. Fang, S. Lv, B. He, Z. Jiang, S. Wei, J. Catal. 255 (2008) 269–278.
[35] S. Carrettin, P. Concepción, A. Corma, J.M. López Nieto, V.F. Puntes, Angew. Chem. Int. Ed. 43 (2004) 2538–2540.
[36] N. Russo, D. Fino, G. Saracco, V. Specchia, Catal. Today 117 (2006) 214–219.
[37] F. Arena, P. Famulari, G. Trunfio, G. Bonura, F. Frusteri, L. Spadaro, Appl. Catal. B: Environ. 66 (2006) 81–91.
[38] L.F. Liotta, G. Di Carlo, A. Longo, G. Pantaleo, A.M. Venezia, Catal. Today 139 (2008) 174–179.
[39] U.R. Pillai, S. Deevi, Appl. Catal. A: Gen. 299 (2006) 266–273.
[40] L.-H. Chang, N. Sasirekha, B. Rajesh, Y.-W. Chen, Sep. Purif. Technol. 58 (2007) 211–218.
[41] A. Wolf, F. Schüth, Appl. Catal. A: Gen. 226 (2002) 1–13.
[42] P. Konova, A. Naydenov, T. Tabakova, D. Mehandjiev, Catal. Commun. 5 (2004) 537–542.
[43] X. Zhang, H. Wang, B.-Q. Xu, J. Phys. Chem. B 109 (2005) 9678–9683.
[44] S.-P. Wang, T.-Y. Zhang, X.-Y. Wang, S.-M. Zhang, S.-R. Wang, W.-P. Huang, S.-H. Wu, J. Mol. Catal. A: Chem. 272 (2007) 45–52.